This is a preprint, the final version is subject to change, of the American Mineralogist (MSA)
Cite as Authors (Year) Title. American Mineralogist, in press.
(DOI will not work until issue is live.) DOI: http://dx.doi.org/10.2138/am.2014.4722

REVISION 2

Crystal chemistry of the ulvöspinel-qandilite series

FERDINANDO BOSI[1], ULF HÅLENIUS[2] AND HENRIK SKOGBY[2]

[1]Dipartimento di Scienze della Terra, Sapienza Università di Roma, Piazzale Aldo Moro 5, I-00185 Roma, Italy

[2]Department of Geosciences, Swedish Museum of Natural History, SE-10405 Stockholm, Sweden

ABSTRACT

Five spinel single-crystal samples within the ulvöspinel-qandilite series [$(Fe_{2-x}Mg_x)TiO_4$, $0.15 < x < 0.94$] were synthesized and structurally and chemically characterized by X-ray diffraction and electron microprobe techniques. Site populations, derived from structural and chemical analysis, show that the tetrahedrally-coordinated site (T) is exclusively populated by Mg^{2+} and Fe^{2+}, while the octahedrally-coordinated site (M) is populated by Ti^{4+}, Mg^{2+}, Fe^{2+} and minor amounts of Fe^{3+}. The inverse cation distribution is characterized by parallel substitution of Mg^{2+} for Fe^{2+} at both the T and M sites along the series.

The variation in the unit-cell parameter from 8.527 Å to 8.495 Å is mainly related to the occurrence of Mg^{2+} at the M site rather than the T site. In fact, the substitution of Mg^{2+} for Fe^{2+} yields significant variations in M-O (from 2.045 Å to 2.034 Å) and only limited variation in T-O (from 2.007 Å to 2.002 Å). In conjunction with data from the literature, the present study provide a basis for quantitative analyses

of the variation in ^{T}Mg-O bond distance from 1.966 Å for Mg-poor ulvöspinel to 1.990 Å for the qandilite end-member.

INTRODUCTION

Several substances such as multiple oxides, sulfides (e.g., $ZnAl_2S_4$), selenides (e.g., $CuCr_2Se_4$), halides (e.g., Li_2NiF_4), and pseudohalides [e.g., $ZnK(CN)_4$] crystallize in the spinel-type structure. Spinel oxides are defined by the general formula AB_2O_4, where A and B are usually cations of either 2+ and 3+ valence ($A^{2+}B^{3+}{}_2O_4$, so-called 2-3 spinels), or of 4+ and 2+ valence ($A^{4+}B^{2+}{}_2O_4$, so-called 4-2 spinels). The spinel structure, typically symmetry $Fd\bar{3}m$, can be described as a slightly distorted cubic close packed array of oxygen anions, in which the A and B cations are distributed in one-eighth of all tetrahedrally-coordinated sites (T) and half of all octahedrally-coordinated sites (M) (e.g., Bragg 1915; Nishikawa 1915). The unit-cell parameters (a) and oxygen fractional coordinates (u, u, u) define the resulting tetrahedral (T-O) and octahedral (M-O) bond lengths (e.g., Lavina et al. 2002). The distribution of A and B cations over T and M sites leads to two different types of cation ordering: (1) normal spinel, where the A cation occupies T and the two B cations occupy M and (2) inverse spinel, where one of the B cations occupies T and the remaining A and B cations occupy M. Disordered cation distributions are often encountered among the 2-3 spinels, and can be described by the general formula $^{T}(A^{2+}{}_{1-i}B^{3+}{}_{i})^{M}(A^{2+}{}_{i}B^{3+}{}_{2-i})O_4$ where i is defined as the inversion parameter. The value of the inversion parameter depends on the spinel composition and cation site preferences: for example, Cr^{3+} only occupies the M site, Al and Cu^{2+} exhibit preference for M, whereas Mg^{2+}, Fe^{2+}, Mn^{2+}, Zn and Co^{2+}

exhibit preference for the T site (Andreozzi et al. 2001; Andreozzi and Lucchesi 2002; Lenaz et al. 2004; Bosi et al. 2010; Hålenius et al. 2011; Fregola et al. 2012; D'Ippolito et al. 2012; Bosi et al. 2012). In addition, the degree of inversion is strongly sensitive to temperature, and at high temperatures (around 1500 °C), the *i*-parameter may increase up to 0.35 for normal spinel and down to 0.70 for inverse spinel (Nell et al. 1989; O'Neill et al. 1992; Redfern et al. 1999; Andreozzi et al. 2000). The temperature dependence of cation ordering/disordering has petrological implications for cooling processes because it is strictly related to the closure temperature of spinel, i.e., the point where the ordering process is effectively quenched. Several studies have addressed this phenomenon (e.g., Princivalle et al. 1989; Della Giusta et al. 1996; Lucchesi and Della Giusta 1997; Lucchesi et al. 1998; Princivalle et al. 1999; Uchida et al. 2005; Lenaz et al. 2010; Lucchesi et al. 2010; Lenaz and Princivalle 2011; Princivalle et al. 2012). Extensive solid-solution occurs between various spinel end-members, particularly among pairs with the same ordering type. For example, spinel (*sensu stricto*)-galaxite $MgAl_2O_4$-$MnAl_2O_4$ is a binary system consisting of two normal spinels (Hålenius et al. 2011), whereas ulvöspinel-qandilite Fe_2TiO_4-Mg_2TiO_4 is a binary system consisting of two inverse spinels (studied hereafter).

The ulvöspinel-qandilite series forms part of the Fe_2TiO_4-Mg_2TiO_4-$FeFe_2O_4$-$MgFe_2O_4$ spinel quadrilateral, and spinels within this compositional field has frequently been utilized as petrogenic indicators of temperature and pressure for geological processes. Thermodynamic data and computational results related to order-disorder phenomena in qandilite and titanomagnetite have been reported in the literature (e.g., O'Neill and Scott 2005; Palin et al. 2008; Lilova et al. 2013; Harrison et al. 2013) as well as several crystal chemical studies (e.g., Wechsler et al. 1984; Wechsler and Von

Dreele 1986; O'Neill et al. 2003; Bosi et al. 2009). However, no systematic investigation of the structural variations all along the entire $(Fe_{2-x}Mg_x)TiO_4$ series has so far been published. In this study, we have investigated the crystal structures of synthetic single crystal spinels belonging to the Fe_2TiO_4-Mg_2TiO_4 series. As most of the physical properties of Ti-rich spinels are very closely related to their cation distribution, the aim of the study was to quantitatively detail the site-occupancy to explore the interplay between chemistry and structure.

EXPERIMENTAL METHODS

Crystal synthesis

Single-crystal spinel samples of five compositions distributed over the $(Fe_{2-x}Mg_x)TiO_4$ join with $0.15 < x < 0.94$ were synthesized by a flux growth method. The samples were grown from saturated melts under slow cooling (4°C/h) from 1200 to 900 °C. In order to maintain a low oxygen fugacity during crystal growth, a continuous flow of CO_2 and H_2 (ratio 1:2) was passed through the furnace tube. Details of the synthesis procedure, using a mixture of BaO and B_2O_3 as flux compound, are described in Bosi et al. (2008). The synthetic products consisted of spinel crystals dispersed in a borate glass. In addition, borate crystals and sometimes ilmenite, rutile, haggertyite ($BaTi_5Fe_6MgO_{19}$), metallic iron and $BaTiO_3$ were also present.

In the present flux-growth experiments, the crystals nucleate and grow somewhere along the main cooling path from 1200 to 900 °C. After 900 °C, the furnace heating power was switched off and the cooling rate was set considerably faster, initially a few hundred degrees per hour, to prevent any substantial crystal growth

during this stage. Consequently, the temperature at which the present samples were last in equilibrium was estimated to be in the range 1000-900 °C and this corresponds to the equilibrium temperature calculated for ulvöspinel single crystal synthetized under the same condition (Bosi et al. 2008).

Several attempts to synthetize single crystal with Mg_2TiO_4 components larger than 50% (i.e., $x > 1$) were unsuccessful. Literature data for the qandilite end-member was therefore also taken into consideration (see section on "Results and discussion").

Single-crystal structural refinement

X-ray diffraction measurements were performed at Earth Sciences Department, Sapienza University of Rome, with a Bruker KAPPA APEX-II single-crystal diffractometer, equipped with a CCD area detector (6.2 × 6.2 cm^2 active detection area, 512 × 512 pixels) and a graphite crystal monochromator, using MoKα radiation from a fine-focus sealed X-ray tube. The sample-to-detector distance was 4 cm. A total of 5088 exposures per sample (step = 0.2°, time/step = 10 s) covering the full reciprocal sphere were collected. The orientation of the crystal lattice was determined from 500 to 1000 strong reflections ($I > 100\ \sigma_I$) evenly distributed in the reciprocal space, and used for subsequent integration of all recorded intensities. Final unit-cell parameters were refined by using the Bruker AXS SAINT program from about 2000 recorded reflections with $I > 10\ \sigma_I$ in the range $8° < 2\theta < 90°$. The intensity data were processed and corrected for Lorentz, polarization and background effects with the APEX2 software program of Bruker AXS. The data were corrected for absorption using multi-scan method (SADABS). The absorption correction led to a significant improvement in R_{int}.

No violation of $Fd\bar{3}m$ symmetry was noted. Sporadic appearance of forbidden space-group reflections was recognized as double reflections.

Structural refinements were carried out with the SHELXL program (Sheldrick 2008). Setting the origin at $\bar{3}m$, initial atomic positions for oxygen atoms were taken from the structure of spinel (Bosi et al. 2009). Variable parameters were overall scale factor, extinction coefficient, atomic coordinates, site scattering values expressed as mean atomic number (m.a.n.), and atomic displacement factors. In accord with the recommendations of Della Giusta et al. (1986) and Hawthorne et al. (1995), to obtain the most accurate results the oxygen site was modeled with partially oxidized scattering factor, ranging from 50% to 60%, derived from neutral *versus* fully ionized oxygen scattering curves. Neutral curves were used for the cation sites: in detail, the T site was modeled considering the presence of Fe and Mg scattering factors, whereas the M site was modeled by Ti, Fe and Mg scattering factors. The final refinements were carried out fixing the occupancy of Ti to the value obtained from the chemical analysis. This approach led to the best values for all conventional statistical indexes, such as $R1$ and $wR2$. Three full-matrix refinement cycles with isotropic displacement parameters for all atoms were followed by anisotropic cycles until convergence was attained, that is, when the shifts for all refined parameters were less than their estimated standard deviation. Table 1 summarizes structural parameters and refinement details, and the corresponding CIFs have been deposited.

Electron microprobe analysis

Electron microprobe analyses, with WDS method, of the same crystals used for XRD refinements were obtained with a Cameca SX50 instrument at the University of

Uppsala operating at an accelerating potential of 20 kV and a sample current of 15 nA. Standard samples were synthetic $MnTiO_3$ (for Ti), Fe_2O_3 (for Fe) and MgO (for Mg). Al_2O_3 was checked, using corundum standard, as a possible contaminant from the furnace tube. Na and Ba contamination from the flux was not detected. For raw data reduction, the PAP matrix correction procedure was applied (Pouchou and Pichoir 1991). The atomic proportions and $Fe^{3+}/\Sigma Fe$ ratios were calculated assuming charge balance and stoichiometry. The assumption of stoichiometric sample compositions is supported by results from previously studied Ti-rich compositions synthesized under similar conditions (Bosi et al. 2008). The results, which are summarized in Table 2, represent mean values of a minimum of six spot analyses per analyzed crystal and their standard errors (below 1%) demonstrate the crystal homogeneity.

Cation distribution

The intracrystalline cation distribution over the T and M sites was obtained by using a least-squares optimization method applying a minimization function in which both structural and chemical data (such as atomic proportions, bond lengths and site-scattering in terms of equivalent electrons, i.e., m.a.n.) were taken into account. The minimization procedure was presented and discussed previously (e.g., Bosi et al. 2009). In particular, octahedral and tetrahedral bond lengths were calculated as the linear contribution of each cation multiplied by its specific bond length. The latter were taken from Lavina et al. (2002): $^{M}Ti^{4+}$-O = 1.962(1) Å, $^{M}Fe^{3+}$-O = 2.015(1) Å, $^{T}Fe^{3+}$-O = 1.875(2) Å, $^{M}Fe^{2+}$-O = 2.150(2) Å, $^{T}Fe^{2+}$-O = 2.006(2) Å, ^{M}Mg-O = 2.082(2) Å, ^{T}Mg-O = 1.966(1) Å, except for $^{T}Fe^{2+}$-O distance which was measured by Bosi et al. (2009) for Fe_2TiO_4. In addition, as explained in more detail below, the value of ^{T}Mg-O distance

varies from 1.966 Å (for Mg-poor ulvöspinel) to 1.990 Å (for qandilite): the former was used for samples T1, T2 and T3, the latter one for samples T4 and T5. The robustness of this approach was confirmed by another optimization procedure (Wright et al. 2000), which led to very similar cation distributions. Results of the final cation distributions are reported in Table 3.

RESULTS AND DISCUSSION

In order to investigate the crystal chemistry of the whole Fe_2TiO_4-Mg_2TiO_4 series, earlier reported data for Mg-free ulvöspinel (FeTib1b, Bosi et al. 2009) and data for Fe-free qandilite (see below) with cubic symmetry were compared with our samples. For sample FeTib1b, the structural formula is $^{T}(Fe^{2+})^{M}(Fe^{2+}_{0.945}Fe^{3+}_{0.11}Ti^{4+}_{0.945})O_4$ and the bond distances are T-O = 2.006(2) Å and M-O = 2.046(1) Å. The structural parameters for qandilite (Mg_2TiO_4) from several studies indicate that the *u* value is in the 0.2616-0.2605 range (Wechsler and von Dreele 1989; Sawada 1996; Millard et al. 1995; O'Neill et al. 2003), whereas the *a* value is in a more limited 8.442-8.444 Å range (O'Neill et al. 2003; Sawada 1996). Therefore, averaged values of $u = 0.2611$ and $a = 8.443$ Å were used herein, which yield M-O = 2.021 Å and T-O = 1.990 Å representative of the end-member $^{T}(Mg^{2+})^{M}(Mg^{2+}Ti^{4+})O_4$.

The investigated synthetic spinels can be represented by the chemical formula $[Fe^{2+}_{(2-x-y/2)}\,Mg^{2+}_{(x)}\,Fe^{3+}_{(y)}\,Ti^{4+}_{(1-y/2)}]_{\Sigma 3.00}\,O_4$ that highlights two types of substitutions: the main $Mg^{2+} \leftrightarrow Fe^{2+}$ exchange with *x* ranging from 0.15 to 0.94, and the minor $Fe^{2+} + Ti^{4+} \leftrightarrow 2Fe^{3+}$ exchange with *y* ranging from 0.13 to 0.04 (sample T1 and T5, respectively). The latter substitution decreases with increasing *x*-value. The cation

193 distribution shows that Ti^{4+} and Fe^{3+} are ordered at the M site, whereas Mg^{2+} and Fe^{2+}
194 are disordered over the T and M sites: in detail, the amounts of Mg^{2+} are slightly smaller
195 for T than for M, whereas the amounts of Fe^{2+} are larger for M than for T (Table 3).
196 Structural refinement results showed that m.a.n. for both the T and M sites decreases
197 with increasing Mg_2TiO_4 component, reflecting the disordered Mg site allocation: T-
198 and M-m.a.n. decrease (from 26 to 21 and from 23 to 20, respectively) with increasing
199 of substitution $Mg^{2+} \rightarrow Fe^{2+}$ as a consequence of the lower atomic number of Mg (Z =
200 12) in relation to Fe (Z = 26). The unit-cell parameter *a* decreases from 8.527 Å to
201 8.495 Å with increasing Mg_2TiO_4 component (Fig. 1). This is related to significant
202 variations in M-O which decreases from 2.045 Å to 2.034 Å, for the studied samples,
203 compared to strongly limited variation in T-O, 2.007-2.002 Å (Fig. 2). The resulting
204 atomic displacement parameters are relatively high for the studied samples (about 0.01
205 A^2), suggesting the likely presence of a static positional disorder due to the mixing of
206 Mg^{2+}/Fe^{2+} and Ti^{4+} over the M-sites. This conclusion is in line with previous studies on
207 ulvöspinel and qandilite (e.g., Wechsler et al. 1984; Millard et al. 1995; Sawada 1996;
208 Bosi et al. 2009). The variations of M-O and T-O as a function of the $^{M}Mg^{2+}$ and $^{T}Mg^{2+}$
209 (respectively) show a strong negative correlation (Fig. 3).

210 As discussed above, the whole ulvöspinel-qandilite series is characterized by the
211 decrease of *a*, M-O and T-O with increasing Mg, accompanied by increasing ^{T}Mg-O
212 distance from 1.966 Å (ulvöspinel) to 1.990 Å (qandilite). Similar variation was also
213 detected for normal spinel along the $MgCr_2O_4$-MgV_2O_4 series (Lavina et al. 2003),
214 where ^{T}Mg-O ranges from 1.966 Å to 1.974 Å. As argued in Lavina et al. (2003), the
215 increase of ^{T}Mg-O may be caused by dragging effects of cations at the M site (V^{3+} and
216 Cr^{3+} in Lavina et al. 2003; Mg, Fe and Ti in our case), responsible for variation in ^{T}Mg-

O, which maintains the structural distortion and provides the shielding between M-cations. In this regard, Bosi et al. (2010) showed that the structural distortion of spinel is strictly related to the mean quadratic elongation <λ> (Robinson et al. 1971) of the MO_6 polyhedron. Calculated values of <λ> for our samples and those of Lavina et al. (2003) show extremely limited variation (1.008-1.009) which supports the analogy between normal and inverse spinel in which increased ^{T}Mg-O values are required by the structure to reduce the cation-cation repulsion between the M sites. A significant shortening of the ^{T}Mg-O distance from 1.983 Å (for Mg_2TiO_4) to 1.967 Å (for $MgCr_2O_4$) was also noted by Sawada (1996), who related this variation to the different degree of ionicity of the ^{T}Mg-O bond in Mg_2TiO_4 and $MgCr_2O_4$.

IMPLICATIONS

The ulvöspinel-qandilite series is closely related to the magnetite-magnesioferrite series, as well as to titanomagnetite (e.g., Harrison et al. 2013), which are the dominant carriers of magnetic remanence in nature and plays a key role to rock magnetic studies. Our finding that Mg^{2+} behaves analogously to Fe^{2+} in these important magnetic minerals, provides new understanding of the nature of cation ordering in the system Fe_2TiO_4-Mg_2TiO_4-$FeFe_2O_4$-$MgFe_2O_4$ and serves as a guide for future petrological and computational studies.

From a crystallographic viewpoint, the present study gives additional insights into the long-range variations in T-O bond distance of divalent cations in the oxide spinel structure: e.g., $^{T}Zn^{2+}$-O about 1.95-1.98 Å (Bosi et al. 2011); $^{T}Co^{2+}$-O about 1.92-1.99 Å (O'Neill 2003; Bosi et al. 2012); $^{T}Mg^{2+}$-O about 1.97-1.99 Å (this study).

241

242

243 **ACKNOWLEDGEMENTS**

244 Financial support from the project PRIN 2010-11 ‘‘GEO-TECH’’, Università
245 Sapienza 2012 “Studio cristallochimico di spinelli appartenenti alle serie $(Mg,Fe)_2TiO_4$,
246 $(Mg,Cu)Al_2O$ e $(Mg,Fe)(Al,Cr)_2O_4$…”, and the Swedish Research Council through the
247 ESF-program EuroMinScI are gratefully acknowledged. We thank the Associate Editor
248 Kristina Lilova, the Technical Editor and two anonymous reviewers for their careful
249 work and their very constructive comments.

250

251

252 **REFERENCES CITED**

253 Andreozzi, G.B., Princivalle, F., Skogby, H., and Della Giusta, A. (2000) Cation
254 ordering and structural variations with temperature in $MgAl_2O_4$ spinel: an X- ray
255 single crystal study. American Mineralogist, 85, 1164–1171. Erratum, 86, 204.
256 Andreozzi, G.B., Lucchesi, S., Skogby, H., and Della Giusta, A. (2001) Composition
257 dependence of cation distribution in some synthetic $(Mg,Zn)(Al,Fe^{3+})_2O_4$
258 spinels. European Journal of Mineralogy, 13, 391-402.
259 Andreozzi, G.B., and Lucchesi, S. (2002) Intersite distribution of Fe^{2+} and Mg in the
260 spinel (sensu stricto)-hercynite series by single-crystal X-ray diffraction.
261 American Mineralogist, 87, 1113-1120.
262 Andreozzi, G.B., and Princivalle, F. (2002) Kinetics of cation ordering in synthetic
263 $MgAl_2O_4$ spinel. American Mineralogist, 87, 838–844.

Bosi, F., Hålenius, U., and Skogby, H. (2008) Stoichiometry of synthetic ulvöspinel single crystals. American Mineralogist, 93, 1312–1316.

Bosi, F., Hålenius, U., and Skogby, H. (2009) Crystal chemistry of the magnetite-ulvöspinel series. American Mineralogist, 94, 181–189.

Bosi, F., Hålenius, U., and Skogby, H. (2010) Crystal chemistry of the $MgAl_2O_4$-$MgMn_2O_4$-$MnMn_2O_4$ system: Analysis of structural distortion in spinel- and hausmannite-type structures. American Mineralogist, 95, 602-607.

Bosi, F., Andreozzi, G.B., Hålenius, U., and Skogby, H. (2011) Zn-O tetrahedral bond length variations in normal spinel oxides. American Mineralogist, 96, 594–598.

Bosi, F., Hålenius, U., D'Ippolito, V., and Andreozzi, G.B. (2012) Blue spinel crystals in the MgAl2O4-CoAl2O4 series: Part II. Cation ordering over short-range and long-range scales. American Mineralogist, 97, 1834–1840.

Bragg, W.H. (1915) The Structure of the Spinel Group of Crystals. Philosophical Magazine, 30, 305-315.

Nishikawa, S. (1915) Structure of Some Crystals of the Spinel Group. Proceedings of the Physico-Mathematical Society of Tokyo, 8, 199-209.

D'Ippolito, V., Andreozzi, G.B., Bosi, F., and Hålenius, U. (2012) Blue spinel crystals in the $MgAl_2O_4$-$CoAl_2O_4$ series: I. Flux growth and chemical characterisation. American Mineralogist, 97, 1828-1833.

Della Giusta, A., Princivalle, F., and Carbonin, S. (1986) Crystal chemistry of a suite of natural Cr-bearing spinels with $0.15 \leq Cr \leq 1.07$. Neues Jahrbuch für Mineralogie Abhandlungen, 155, 319.330.

Della Giusta, A., Carbonin, S., and Ottonello, G. (1996) Temperature-dependent disorder in a natural Mg-Al-Fe^{2+}-Fe^{3+}-spinel. Mineralogical Magazine, 60, 603–616.

Fregola, R.A., Bosi, F., Skogby, S., and Hålenius, U. (2012) Cation ordering over short-range and long-range scales in the $MgAl_2O_4$-$CuAl_2O_4$ series. American Mineralogist, 97, 1821-1827.

Harrison, R.J., Palin, E.J., and Perks, N. (2013) A computational model of cation ordering in the magnesioferrite-qandilite ($MgFe_2O_4$-Mg_2TiO_4) solid solution and its potential application to titanomagnetite (Fe_3O_4-Fe_2TiO_4). American Mineralogist, 98, 698-708.

Hawthorne, F.C., Ungaretti, L., and Oberti, R. (1995) Site populations in minerals: terminology and presentation of results. Canadian Mineralogist, 33, 907-911.

Hålenius, U., Bosi, F., and Skogby, H. (2011) A first record of strong structural relaxation of TO_4 tetrahedra in a spinel solid solution. American Mineralogist 96, 617-622.

Lavina, B., Salviulo, G., and Della Giusta, A. (2002) Cation distribution and structure modeling of spinel solid solutions. Physics and Chemistry of Minerals, 29, 10-18.

Lavina, B., Reznitskii, L.Z., and Bosi, F. (2003) Crystal chemistry of some Mg, Cr, V normal spinels from Sludyanka (Lake Baikal, Russia): the influence of V^{3+} on structural stability. Physics and Chemistry of Minerals, 30, 599-605.

Lenaz, D., Skogby, H., Princivalle, F., and Hålenius, U. (2004) Structural changes and valence states in the $MgCr_2O_4$-$FeCr_2O_4$ solid solution series. Physics and Chemistry of Minerals, 31, 633-642.

Lenaz, D., De Min, A., Garuti, G., Zaccarini, F., and Princivalle, F. (2010) Crystal chemistry of Cr-spinels from the lherzolite mantle peridotite of Ronda (Spain). American Mineralogist, 95, 1323–1328.

Lenaz, D., and Princivalle, F. (2011) First occurrence of titanomagnetites from the websterite dykes within Balmuccia peridotite (Ivrea-Verbano zone): crystal chemistry and structural refinement. Periodico di Mineralogia, 80, 19-26.

Lilova, K.I., Pearce, C., Gorski, C., Rosso, K.M., and Navrotsky, A. (2012) Thermodynamics of the magnetite-ulvöspinel (Fe_3O_4-Fe_2TiO_4) solid solution. American Mineralogist, 97, 1330–1338.

Lucchesi, S., and Della Giusta, A. (1997) Crystal chemistry of a highly disordered Mg-Al natural spinel. Mineralogy and Petrology, 59, 91-99.

Lucchesi, S., Bosi, F., and Pozzuoli, A. (2010) Geothermometric study of Mg-rich spinels from the Somma-Vesuvius volcanic complex (Naples, Italy). American Mineralogist, 95, 617-621.

Lucchesi, S., Amoriello, M., and Della Giusta, A. (1998) Crystal chemistry of spinels from xenoliths of the Alban Hills volcanic region. European Journal of Mineralogy, 10, 473–482.

Millard, R.L., Peterson, R.C., and Hunter, B.K. (1995) Study of the cubic to tetragonal transition in Mg_2TiO_4 and Zn_2TiO_4 spinels by ^{17}O MAS NMR and Rietveld refinement of X-ray diffraction data. American Mineralogist, 80, 885–896.

Nell, J., Wood, B.J., and Mason, T.O. (1989) High temperature cation distributions in Fe_3O_4-$MgAl_2O_4$-$MgFe_2O_4$-$FeAl_2O_4$ spinels from thermopower measurements. American Mineralogist, 74 , 339-35l.

O'Neill H.St.C., Annersten, H., and Virgo D. (1992) The temperature dependence of the cation distribution in magnesioferrite ($MgFe_2O_4$) from powder XRD structural refinements and Mössbauer spectroscopy. American Mineralogist, 77,725-740.

O'Neill, H.St.C. (2003) The influence of next nearest neighbours on cation radii in spinels: the example of the Co3O4-CoCr2O4 solid solution. Mineralogical Magazine, 67, 547–554.

O'Neill, H.St.C., and Scott, D.R. (2005) The free energy of formation of Mg_2TiO_4 (synthetic qandilite), an inverse spinel with configurational entropy. European Journal of Mineralogy, 7, 315-323.

O'Neill, H.St.C., Redfern, S.A.T., Kesson, S., and Short, S. (2003) An in situ neutron diffraction study of cation disordering in synthetic qandilite Mg_2TiO_4 at high temperatures. American Mineralogist, 88, 860–865.

Palin, E.J., Walker, A.M., and Harrison, R.J. (2008) A computational study of order-disorder phenomena in Mg_2TiO_4 spinel (qandilite). American Mineralogist, 93, 1363–1372.

Pouchou, J.L., and Pichoir, F. (1984) A new model for quantitative X-ray micro-analysis. I. Application to the analysis of homogeneous samples. La Recherche Aérospatiale, 3, 13-36.

Princivalle, F., Della Giusta, A., and Carbonin, S. (1989) Comparative crystal chemistry of spinels from some suites of ultramafic rocks. Mineralogy and Petrolology, 40, 117-126.

Princivalle, F., Della Giusta, A., De Min, A., and Piccirillo, E.M. (1999) Crystal chemistry and significance of cation ordering in Mg-Al rich spinels from high

grade hornfels (Predazzo-Monzoni, NE Italy). Mineralogical Magazine, 63, 257–262.

Princivalle, F., Martignago F., Nestola, F., and Dal Negro A. (2012) Kinetics of cation ordering in synthetic $Mg(Al, Fe^{3+})_2O_4$ spinels. European Journal of Mineralogy, 24, 633-643.

Redfern, S.A.T., Harrison, R.J., O'Neill, H.St.C., and Wood, D.R.R. (1999) Thermodynamics and kinetics of cation ordering in $MgAl_2O_4$ spinel up to 1600°C from in situ neutron diffraction. American Mineralogist, 84, 299-310.

Robinson, K., Gibbs, G.V., and Ribbe, P.H. (1971) Quadratic elongation: A quantitative measure of distortion in coordination polyhedra. Science, 172, 567–570.

Sawada, H. (1996) Electron density study of spinels: magnesium titanium oxide (Mg_2TiO_4). Materials Research Bulletin, 31, 355–360.

Sheldrick, G.M. (2008) A short history of SHELX. Acta Crystallographica, A64, 112-122.

Uchida, H., Lavina, B., Downs, R.T., and Chesley, J. (2005) Single-crystal X-ray diffraction of spinels from the San Carlos Volcanic Field, Arizona: Spinel as a geothermometer. American Mineralogist, 90, 1900-1980.

Wechsler, B.A., and Von Dreele, R.B. (1989) Structure refinement of Mg_2TiO_4,$MgTiO_3$ and $MgTi_2O_5$ by time-of-flight neutron powder diffraction. Acta Crystallographica, B45, 542–549.

Wechsler, B.A., Lindsley, D.H., and Prewitt, C.T. (1984) Crystal structure and cation distribution in titanomagnetites ($Fe_{3-x}Ti_xO_4$). American Mineralogist, 69, 754-770.

379 Wright, S.E., Foley, J.A., and Hughes, J.M. (2000) Optimization of site occupancies in
380 minerals using quadratic programming. American Mineralogist, 85, 524–531.
381

LIST OF TABLES

LIST OF FIGURES AND FIGURE CAPTIONS

FIGURE 1. Unit-cell parameter against mole fraction Mg_2TiO_4 in the ulvöspinel-qandilite series. Symbol dimensions are proportional to 2σ. "ULV" refers to the ulvöspinel end-member (Bosi et al., 2009). "QAND" refers to average data for the qandilite end-member (see text).

FIGURE 2. Variations in T-O (black circles) and M-O (black squares) bond lengths *versus* the unit-cell parameter in the $(Fe,Mg)_2TiO_4$ series. Symbol dimensions and error bars, where shown, are proportional to 2σ. "ULV" and "QAND" as in Figure 1.

FIGURE 3. (a) M-O distance *versus* Mg content at the M site, (b) T-O distance *versus* Mg content at the T site in the $(Fe,Mg)_2TiO_4$ series. Error bars are proportional to 2σ. "ULV" and "QAND" as in Figure 1.

TABLE 1. Selected X-ray diffraction data for the synthetic spinels $(Mg,Fe)_2TiO_4$

Sample	T1	T2	T3	T4	T5
Crystal size (mm)	0.12 × 0.10 × 0.08	0.20 × 0.18 × 0.10	0.10 × 0.09 × 0.08	0.10 × 0.10 × 0.09	0.15 × 0.14 × 0.10
a (Å)	8.5271(3)	8.5184(3)	8.5104(3)	8.5021(3)	8.4946(3)
u	0.26064(6)	0.26099(7)	0.26086(5)	0.26097(7)	0.26108(9)
T-O (Å)	2.0034(9)	2.0065(11)	2.0027(8)	2.0023(10)	2.0022(13)
M-O (Å)	2.0451(5)	2.0403(6)	2.0393(4)	2.0365(5)	2.0339(7)
T-m.a.n.	25.5(2)	25.0(3)	23.7(2)	22.1(2)	21.1(2)
M-m.a.n.	23.4(2)	22.6(3)	21.5(1)	20.5(1)	20.1(2)
T-U^{11} (Å^2)	0.01089(10)	0.01118(13)	0.01090(10)	0.01091(12)	0.01081(18)
M-U^{11} (Å^2)	0.00848(7)	0.00859(9)	0.00851(7)	0.00835(9)	0.00853(12)
M-U^{12} (Å^2)	–0.00060(3)	–0.00077(4)	–0.00072(4)	–0.00079(4)	–0.00086(5)
O-U^{11} (Å^2)	0.0146(2)	0.0143(3)	0.01399(18)	0.0136(2)	0.0132(3)
O-U^{12} (Å^2)	–0.00316(14)	–0.00313(16)	–0.00285(13)	–0.00284(15)	–0.00269(18)
Reciprocal space range *hkl*	$-13 \le h \le 16$	$-14 \le h \le 16$	$-12 \le h \le 16$	$-13 \le h \le 16$	$-16 \le h \le 11$
	$-13 \le k \le 16$	$-13 \le k \le 16$	$-13 \le k \le 16$	$-14 \le k \le 16$	$-14 \le k \le 15$
	$-16 \le l \le 12$	$-12 \le l \le 16$	$-16 \le l \le 12$	$-12 \le l \le 16$	$-16 \le l \le 14$
EXTI	0.0074(4)	0.0170(9)	0.0206(7)	0.0057(5)	0.0089(9)
Read reflections	2838	2845	2845	2919	2850
Unique reflections	151	151	151	148	148
R int. (%)	1.68	2.02	2.09	1.64	3.74
*R*1 all (%)	1.18	1.33	1.10	1.36	1.62
*wR*2 (%)	2.66	3.23	2.33	3.14	4.36
GooF	1.178	1.228	1.219	1.348	1.400
Diff. Peaks (*e*/Å^3)	–0.38; 0.68	–0.44; 1.16	–0.25; 0.23	–0.34; 0.64	–0.25; 1.15

Notes: a = unit-cell parameter; u = oxygen fractional coordinate; T-O and M-O = tetrahedral and octahedral bond lengths, respectively; T- and M-m.a.n.. = T- and M-mean atomic number; U^{11} = atomic displacement parameter; $U^{11} = U^{22} = U^{33}$ and $U^{12} = U^{13} = U^{23}$ (= 0 for T-site due to symmetry reasons); EXTI = extinction parameter; $R_{int.}$ = merging residual value; R1 = discrepancy index, calculated from F-data; wR2 = weighted discrepancy index, calculated from F^2-data; GooF = goodness of fit; Diff. Peaks = maximum and minimum residual electron density. Radiation, Mo-Kα = 0.71073 Å. Data collection temperature = 293 K. Range for data collection 8° < 2θ < 90°. Total number of frames = 5088. Origin fixed at $\bar{3}m$. Space group $Fd\bar{3}m$. Z = 8 formula units. Spinel structure has cations at Wyckoff positions 8a ≡ T (1/8, 1/8, 1/8) and 16d ≡ M (1/2, 1/2, 1/2), and oxygen anions at 32e (u, u, u).

TABLE 2. Chemical composition of the synthetic spinels $(Fe,Mg)_2TiO_4$

Sample	T1	T2	T3	T4	T5
TiO_2 (wt%)	33.98(10)	35.37(10)	36.97(11)	39.54(29)	40.18(11)
MgO	2.78(14)	6.37(5)	10.13(8)	16.31(15)	19.49(28)
FeO_{total}	62.46(42)	58.17(24)	52.74(18)	43.98(31)	40.06(24)
Total	99.22	99.91	99.84	99.84	99.73
FeO*	58.27	54.24	49.88	42.69	38.38
Fe_2O_3*	4.66	4.37	3.184	1.43	1.87
Ti^{4+} (apfu)	0.936(5)	0.942(3)	0.959(3)	0.982(6)	0.977(5)
Mg^{2+}	0.152(8)	0.336(2)	0.521(4)	0.803(6)	0.939(9)
Fe^{2+}	1.784(7)	1.606(4)	1.438(4)	1.179(7)	1.038(6)
Fe^{3+}	0.128(10)	0.116(5)	0.083(5)	0.036(10)	0.045(10)
Total	3.000	3.000	3.000	3.000	3.000

Notes : Cations on the basis of 4 oxygen atoms per formula unit (apfu). Digits in brackets are standard uncertainties (1σ): for reported oxide concentrations, they represent standard deviations of several analyses on individual crystals, while, for cations, they were calculated according to error propagation theory.
* Determined from stoichiometry.

TABLE 3. Structural formulae for the synthetic spinels $(Fe,Mg)_2TiO_4$

Sample	Formula
T1	$^{T}(Mg_{0.03}Fe^{2+}_{0.97})\ ^{M}(Mg_{0.13}Fe^{2+}_{0.80}Fe^{3+}_{0.13}Ti^{4+}_{0.94})O_4$
T2	$^{T}(Mg_{0.07}Fe^{2+}_{0.93})\ ^{M}(Mg_{0.26}Fe^{2+}_{0.68}Fe^{3+}_{0.12}Ti^{4+}_{0.94})O_4$
T3	$^{T}(Mg_{0.16}Fe^{2+}_{0.84})\ ^{M}(Mg_{0.36}Fe^{2+}_{0.59}Fe^{3+}_{0.09}Ti^{4+}_{0.96})O_4$
T4	$^{T}(Mg_{0.28}Fe^{2+}_{0.72})\ ^{M}(Mg_{0.52}Fe^{2+}_{0.46}Fe^{3+}_{0.04}Ti^{4+}_{0.98})O_4$
T5	$^{T}(Mg_{0.35}Fe^{2+}_{0.65})\ ^{M}(Mg_{0.59}Fe^{2+}_{0.39}Fe^{3+}_{0.04}Ti^{4+}_{0.98})O_4$

Notes: T = tetrahedrally coordinated site; M = octahedrally coordinated site

FIGURE 1

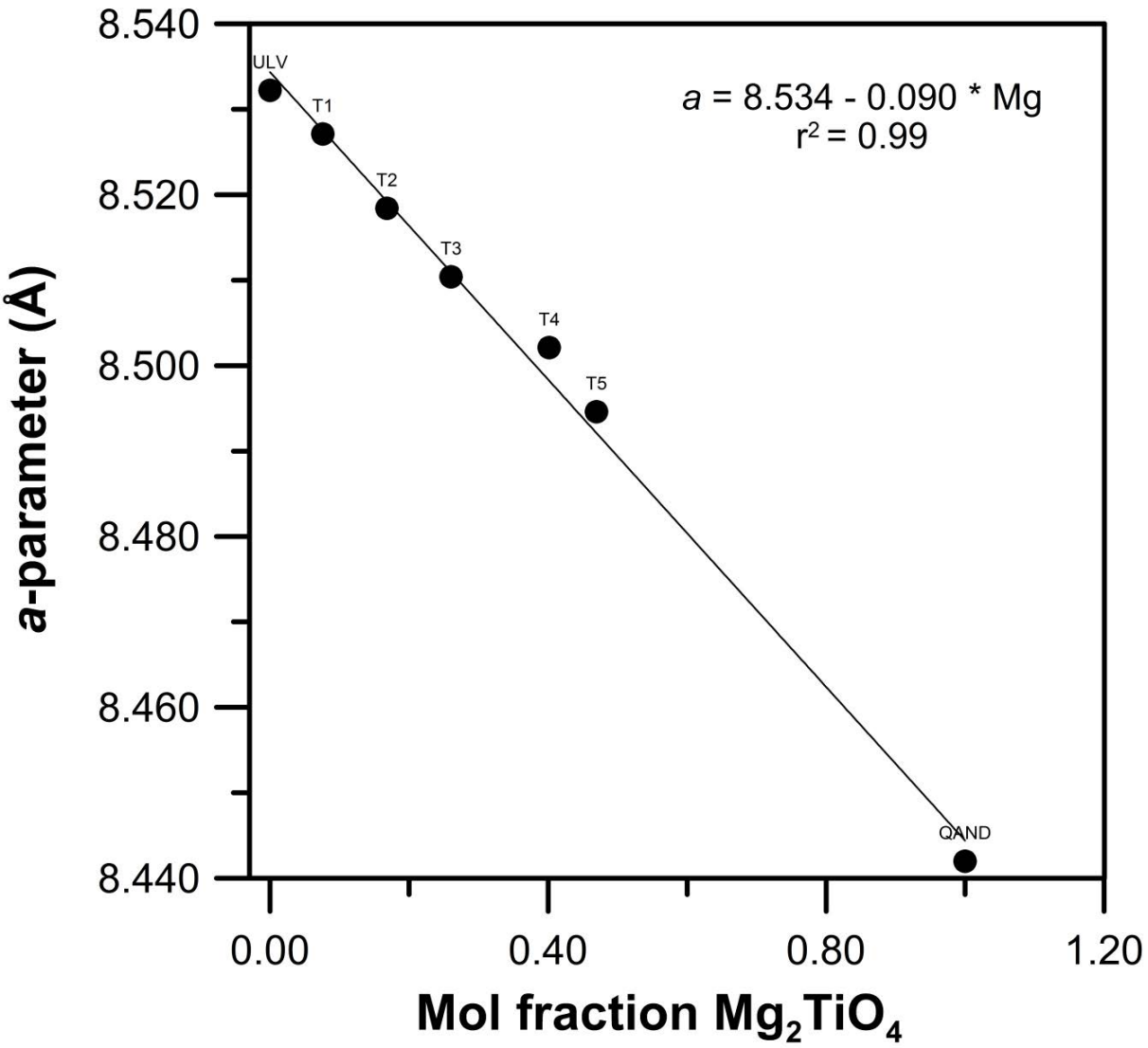
8.540
8.520
8.500
8.480
8.460
8.440
a-parameter (Å)
ULV
T1
T2
T3
T4
T5
QAND
a = 8.534 - 0.090 * Mg
r2 = 0.99
0.00
0.40
0.80
1.20
Mol fraction Mg2TiO4

FIGURE 2

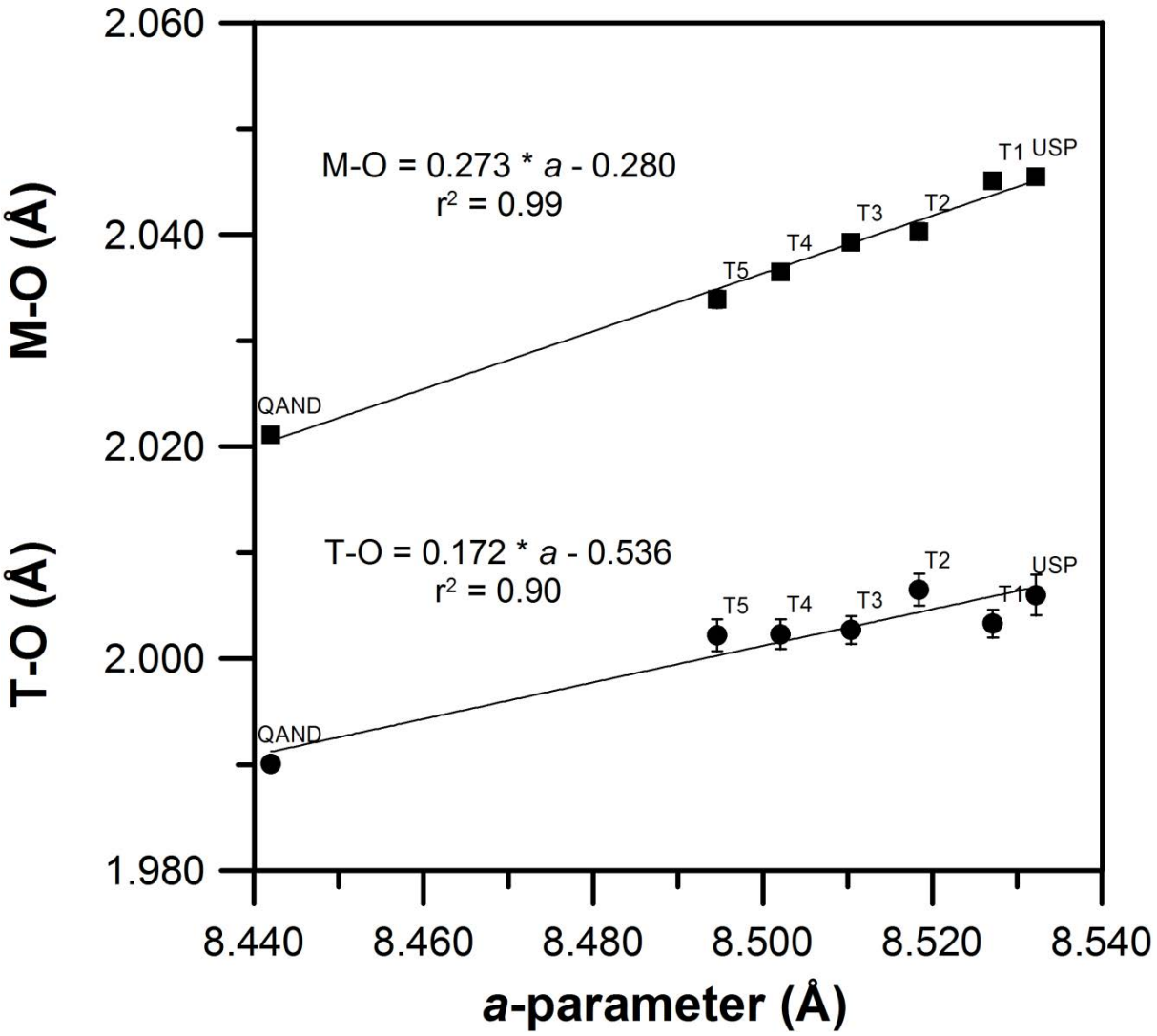
M-O = 0.273 * a - 0.280
r2 = 0.99
T-O = 0.172 * a - 0.536
r2 = 0.90
M-O (Å)
T-O (Å)
a-parameter (Å)
2.060
2.040
2.020
2.000
1.980
8.440
8.460
8.480
8.500
8.520
8.540
QAND
T5
T4
T3
T2
T1
USP

FIGURE 3a

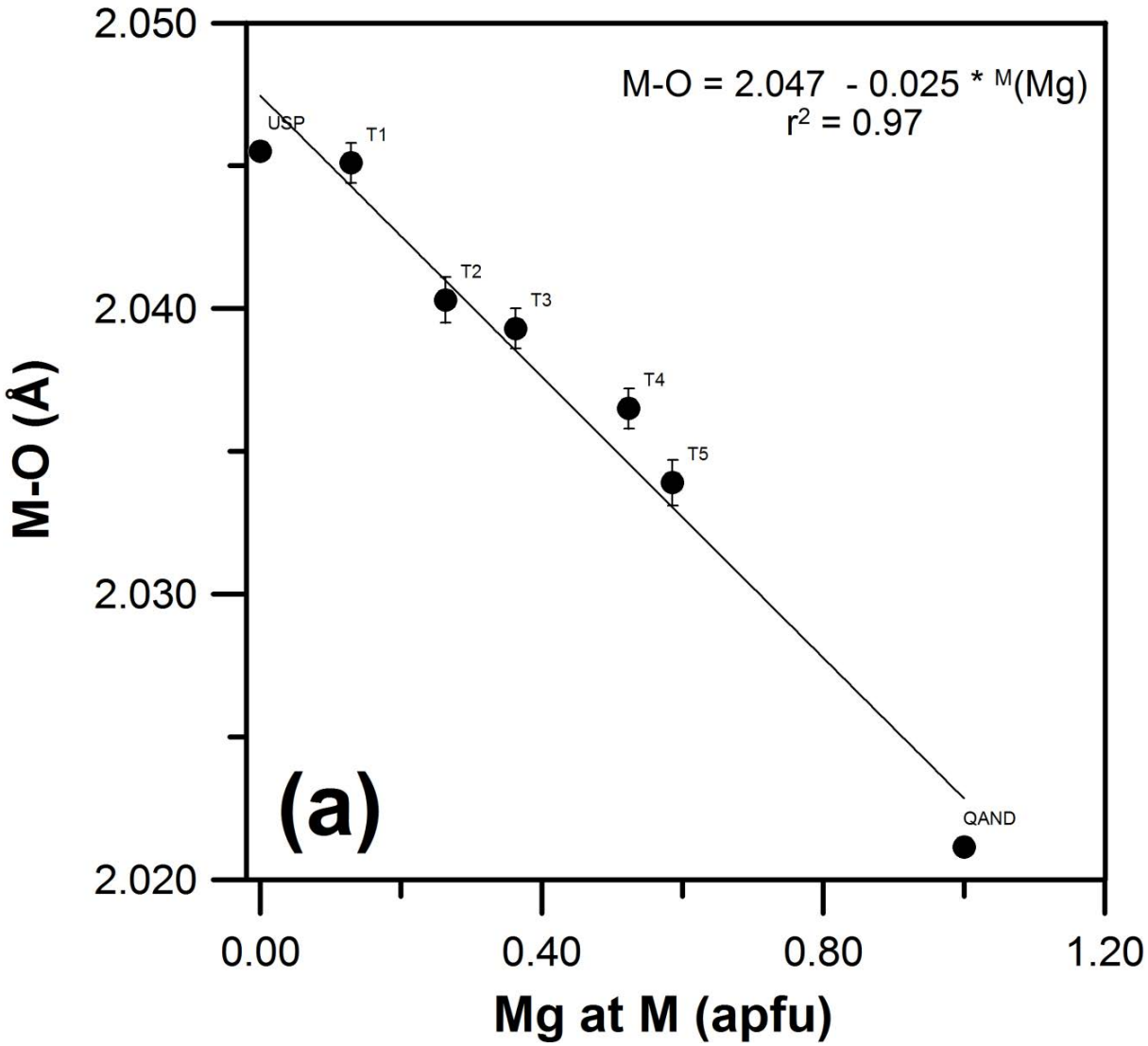
M-O = 2.047 - 0.025 * M(Mg)
r2 = 0.97
USP
T1
T2
T3
T4
T5
QAND
(a)
M-O (Å)
2.050
2.040
2.030
2.020
0.00
0.40
0.80
1.20
Mg at M (apfu)

FIGURE 3b

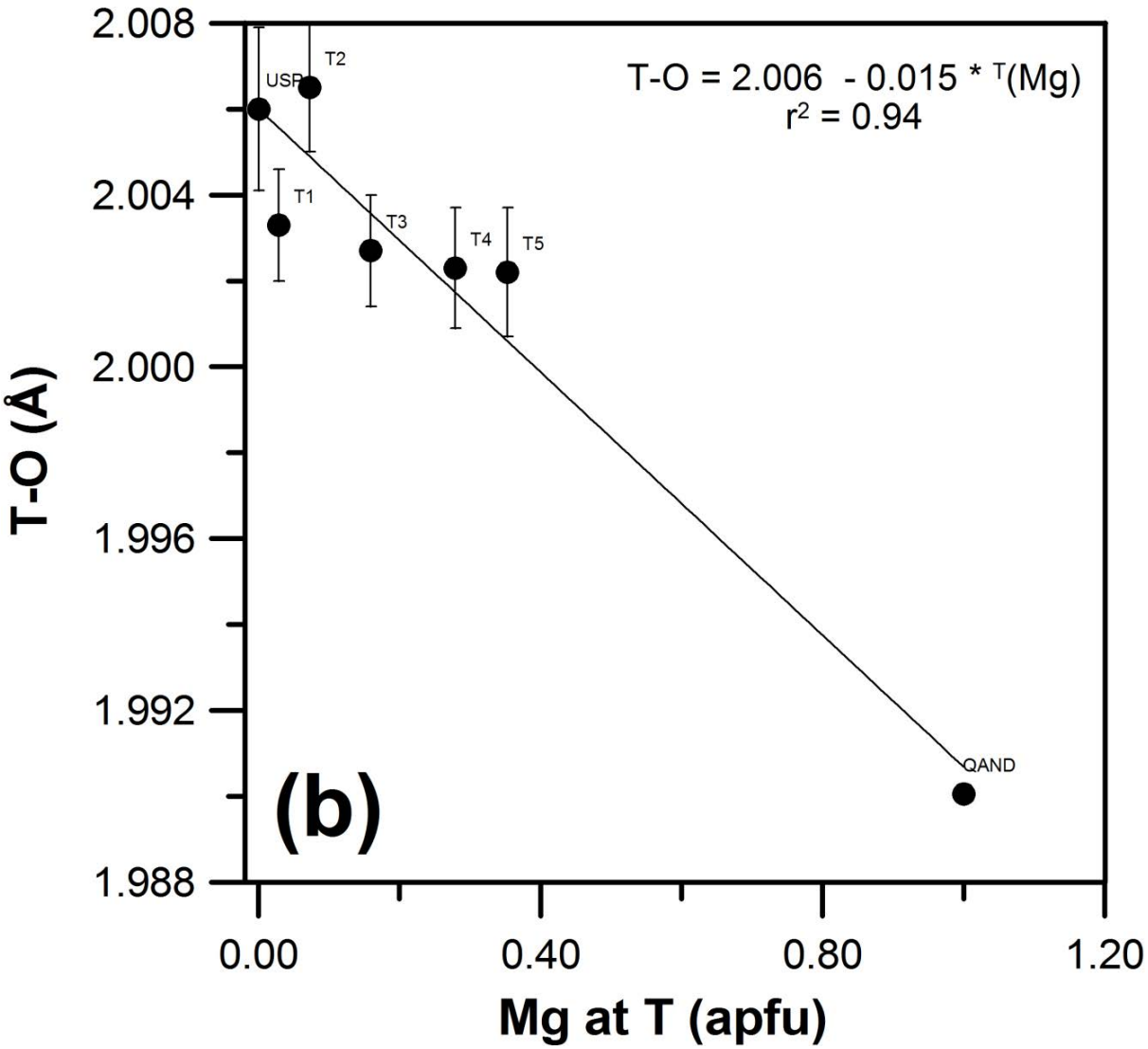
T-O = 2.006 - 0.015 * T(Mg)
r2 = 0.94
USR
T2
T1
T3
T4
T5
QAND
(b)
T-O (Å)
2.008
2.004
2.000
1.996
1.992
1.988
0.00
0.40
0.80
1.20
Mg at T (apfu)